Chemistry Europe
European Chemical Societies Publishing

WILEY VCH

Excellence in Chemistry Research

Announcing our new flagship journal

- Gold Open Access
- Publishing charges waived
- Preprints welcome
- Edited by active scientists

Meet the Editors of *ChemistryEurope*

Luisa De Cola
Università degli Studi di Milano Statale, Italy

Ive Hermans
University of Wisconsin-Madison, USA

Ken Tanaka
Tokyo Institute of Technology, Japan

Medicinal Chemistry & Drug Discovery

Synthesis, Characterization, Antimicrobial Evaluation, and Computational Investigation of Substituted Imidazo[2,1-*b*][1,3,4]Thiadiazole Derivatives

Meltem Dagli,[a] Mustafa Er,[a] Tuncay Karakurt,[b] Abdurrahman Onaran,[c] Hakan Alici,[d] and Hakan Tahtaci*[a]

In this study, a novel series of 2,6-disubstituted and 2,5,6-trisubstituted imidazo[2,1-*b*][1,3,4]thiadiazole derivatives were synthesized starting from 2-amino-1,3,4-thiadiazole derivatives. Structures of the synthesized compounds were characterized using various analysis techniques. Then, in vitro biological activity tests were carried out for all synthesized compounds and they were found to show moderate to good activity against all bacteria and fungi tested. Next, molecular docking simulations were performed to observe the inhibition effect of the synthesized compounds on the 3R9C receptor and support their biological activity results. Finally, the pharmacokinetic, ADME and toxicity properties of all compounds were examined using FAF-Drugs and ProTox webservers and it was concluded that they had acceptable toxicity and ADME properties.

1. Introduction

Recently, there has been increasing interest in drug active ingredients, and the number of studies aimed at the diversification of methods to synthesize these types of substances has been increasing, as well. Briefly, the main reasons for the high number of studies on and the increasing interest in such drug active ingredients include the increasing number of viral diseases and constantly mutating viral strains, adverse effects of factors associated with environmental pollution on the human immune system, and the high toxicity of existing drug active ingredients.[1] For these reasons, scientists are making great efforts to design drug active ingredients against constantly evolving diseases with low cost, high efficiency, minimal toxicity, and maximal bioavailability.

Compounds that contain one or more heteroatoms other than carbon and hydrogen such as oxygen, nitrogen, or sulfur and have the maximum number of conjugated double bonds such as imidazole and thiadiazole are referred to as heterocyclic compounds.[2] As it is well-known that heterocyclic compounds exhibit a wide range of biological activities.[3] Such compounds therefore have an important role for life. What makes heterocyclic compounds even more important is that they are not only found in the natural environment but can also be obtained synthetically.

Imidazole, 1,3,4-thiadiazole, and their derivatives are among the heterocyclic compounds used in clinical practice, in commercial drugs, and in many fields such as materials science. Therefore, studies on the synthesis, characterization, and biological activity of imidazole, 1,3,4-thiadiazole, and the derivatives of these compounds are being intensively pursued.[4–7] Thiadiazole is a heterocyclic aromatic compound with a five-member ring with two nitrogen atoms and one sulfur atom. This compound has four different isomeric forms found in nature: 1,2,3-thiadiazole, 1,2,4-thiadiazole, 1,2,5-thiadiazole, and 1,3,4-thiadiazole. Of these isomers, 1,3,4-thiadiazole and its derivatives are highly reactive to nucleophilic substitution reactions and exhibit a wide range of biological activities; these compounds therefore have been synthesized increasingly, particularly in recent years.[8,9]

Imidazole is another heterocyclic aromatic compound with the formula $C_3H_4N_2$. Imidazole and its derivatives are also widely studied in the field of pharmaceutical chemistry due to their versatile use and various biological activities.[10]

Heterocyclic systems in which imidazole and 1,3,4-thiadiazole rings are fused to each other with a bridgehead nitrogen atom are referred to as imidazo[2,1-*b*][1,3,4]thiadiazoles.[11–13] Imidazo[2,1-b][1,3,4]thiadiazoles and their derivatives have become widely used compounds in pharmaceutical chemistry due to their broad spectrum of biological activities such as antimicrobial, antibacterial, antifungal, antiviral, antioxidant, anticonvulsant, antidepressant, anti-inflammatory, antituberculosis, antihypertensive, and antiproliferative activities.[14–26] Moreover, synthesis of these compounds and their derivatives has also become a focus of interest in anticancer activity

[a] *M. Dagli, Prof. M. Er, Dr. H. Tahtaci*
Department of Chemistry, Faculty of Science, Karabuk University, 78050, Karabuk, Turkey
Fax: +90 370 418 72 62
Tel: +90 370 418 72 60
E-mail address:
E-mail: hakantahtaci@karabuk.edu.tr
[b] *Dr. T. Karakurt*
Department of Chemical Engineering, Faculty of Engineering and Architecture, Kırşehir Ahi Evran University, 40100, Kırşehir, Turkey
[c] *Dr. A. Onaran*
Department of Plant and Animal Production, Kumluca Vocational School of Higher Education, Akdeniz University 07350, Antalya, Turkey
[d] *Dr. H. Alici*
Department of Physics, Faculty of Arts and Sciences, Zonguldak Bulent Ecevit University, 67100, Zonguldak, Turkey

Supporting information for this article is available on the WWW under https://doi.org/10.1002/slct.202002821

Table 1. Mycelial growth against plant pathogenic fungi.

Compounds	Mycelial growth (mm) *Rhizoctonia solani* Doses (μg/mL) 2000	4000	*Alternaria alternata* Doses (μg/mL) 2000	4000
C-	60.00 ± 0.00		60.00 ± 0.00	
5a	12.4[a] ± 0.6	8.8 ± 0.7	27.4 ± 1.3	18.5 ± 0.4
5b	14.9 ± 1.5	6.1 ± 0.2	25.8 ± 0.6	18.2 ± 1.9
5c	18.7 ± 1.1	10.5 ± 0.3	31.8 ± 1.6	17.8 ± 1.0
5d	12.6 ± 1.1	7.3 ± 0.6	34.3 ± 0.9	19.6 ± 0.6
5e	13.0 ± 1.3	8.2 ± 1.1	38.5 ± 0.5	26.2 ± 0.7
5f	12.6 ± 1.9	8.4 ± 0.9	16.9 ± 1.1	11.8 ± 1.1
5g	18.9 ± 1.3	8.4 ± 1.1	31.8 ± 1.2	18.1 ± 0.8
5h	24.1 ± 1.9	13.6 ± 1.8	15.6 ± 0.6	22.5 ± 1.1
5i	17.2 ± 0.7	11.7 ± 1.4	17.6 ± 1.5	15.0 ± 0.9
5k	30.8 ± 1.2	15.7 ± 1.5	33.6 ± 1.1	24.1 ± 2.2
6a	22.8 ± 2.0	16.4 ± 0.1	30.8 ± 1.5	25.9 ± 1.2
6b	26.2 ± 0.6	15.6 ± 0.8	25.3 ± 1.1	14.2 ± 1.4
7a	19.3 ± 0.7	14.6 ± 1.2	38.9 ± 1.3	19.3 ± 1.7
7b	15.5 ± 1.2	12.7 ± 1.9	26.5 ± 0.5	17.1 ± 1.5
8a	12.6 ± 0.7	15.8 ± 0.8	29.1 ± 1.2	17.8 ± 1.1
8b	23.9 ± 1.1	12.9 ± 0.6	18.8 ± 2.5	9.2 ± 1.8
10	26.4 ± 0.8	16.8 ± 0.3	23.1 ± 0.4	9.9 ± 1.2
11	22.9 ± 2.6	15.6 ± 0.9	26.9 ± 0.7	7.8 ± 0.8
12	20.8 ± 1.4	10.3 ± 1.2	26.8 ± 0.6	16.7 ± 0.9
13	20.1 ± 1.3	14.7 ± 0.1	25.1 ± 0.8	14.4 ± 1.1
16	17.0 ± 1.4	12.3 ± 0.6	30.3 ± 1.7	15.3 ± 1.1
17	20.9 ± 0.3	10.8 ± 0.6	32.1 ± 1.8	16.7 ± 1.7
18	22.3 ± 1.9	14.0 ± 1.2	28.5 ± 1.5	13.6 ± 1.0
19	29.8 ± 1.2	15.2 ± 1.8	12.4 ± 1.3	5.9 ± 0.3
C+	0 ± 0.00		0 ± 0.00	

Mycelial growth (MG) ± Standard deviation (SD), C+: Positive control (Thiram), C-: Negative control (DMSO).[a] Mean of three assays.

studies due to their similar structure to levamisole, tetramisole, and dexamisole, which are good immune system effectors.[27,28]

In addition to these heterocyclic aromatic compounds, aliphatic heterocyclic compounds such as morpholine, piperidine, and pyrrolidine are other examples of bioactive compounds used in many fields and pharmaceutical chemistry in particular.[29–33]

In light of the significant literature data mentioned above, the main purpose of this study is to synthesize 2,6-disubstituted and 2,5,6-trisubstituted imidazo[2,1-*b*][1,3,4]thiadiazole derivatives, to characterize these compounds using various spectroscopic methods, and to investigate their antimicrobial activity.

Another aim of this study, by using various theoretical approaches, is to elucidate the drug-likeness properties of the compounds synthesized and to support their experimental activity results. For this purpose, the pharmacokinetics, ADME and toxicity analyzes were evaluated according to Lipinski rules and FAF-Drugs standards. Moreover, the inhibition effects of synthesized compounds on the 3R9C receptor were investigated using molecular docking simulations, thereby supporting the experimental activity results and identifying possible binding regions of all compounds on the receptor.

2. Results and discussion

2.1. Chemistry

In this study on the synthesis, characterization, and biological activity of Mannich bases of imidazo[2,1-*b*][1,3,4]thiadiazole and some theoretical calculations, 12 new 2,6-disubstituted imidazo[2,1-*b*][1,3,4]thiadiazole derivatives (**5a**–**k**, **10**, and **16**) as well as 12 new 2,5,6-trisubstituted imidazo[2,1-*b*][1,3,4] thiadiazole derivatives (compounds **6a**–**b**, **7a**-**b**, **8a**-**b**, **11**–**13**, and **17**–**19**) were synthesized as target compounds. The compounds were synthesized using the synthetic routes shown in Schemes 1–3.

The starting compounds, 2-amino-1,3,4-thiadiazole derivatives (compounds **3**, **9**, and **15**), were synthesized in the first part of the study. Compounds **3** and **9** were obtained from the reactions of 5-amino-1,3,4-thiadiazole-2-thiol (**2**) with 2,4-dichlorobenzylchloride (**1**) and 4-fluorobenzylchloride (**8**) in the presence of KOH with high yields (88% and 89%), as indicated in the literature.[34–36] The other starting compound, compound **15**, was synthesized from the reaction of nitrile compound (**14**) with thiosemicarbazide in trifluoroacetic acid (TFA) at 60 °C with a high yield (88%).[37] In this reaction, the nucleophilic attack of thiosemicarbazide to the imine carbon occurs first under the catalytic effect of TFA. It is believed that the elimination of the ammonia ion and the sulfur's nucleophilic

Table 2. Percentage inhibition (%) against tested fungi.

Compounds	*Rhizoctonia solani* Doses (μg/mL) 2000	4000	*Alternaria alternata* Doses (μg/mL) 2000	4000
C-	–	–	–	–
5a	79	85	54	69
5b	75	90	57	70
5c	69	83	47	70
5d	79	88	43	67
5e	78	86	36	56
5f	79	86	72	80
5g	69	86	47	70
5h	60	77	74	63
5i	71	80	71	75
5k	49	74	44	60
6a	62	73	49	57
6b	56	74	58	76
7a	68	76	35	68
7b	74	79	56	71
8a	79	74	52	70
8b	60	78	69	85
10	56	72	62	83
11	62	74	55	87
12	65	83	55	72
13	67	75	58	76
16	72	79	49	75
17	65	82	47	72
18	63	77	53	77
19	50	75	79	90
C+	100	100	100	100

(–): No percentage inhibition, C+: Positive control (Thiram), C-: Negative control (DMSO).

Table 3. Antifungal activity values (LD_{50}, MFC, and MIC) against tested fungi.

Compounds	(LD_{50}[a]/MFC[b]/ MIC[c] μg/mL) *Rhizoctonia solani*	*Alternaria alternata*
5a	963/ > 4000/62.5	1688/ > 4000/ < 31.25
5b	664/ < 2000/125	2021/ > 4000/125
5c	1445/ > 4000/ > 31.25	1862/ > 4000/ < 31.25
5d	1229/ > 2000/125	2222/ > 2000/ > 125
5e	1305/ > 4000/62.5	2981/ > 4000/ < 31.25
5f	907/ < 2000/ < 31.25	1397/ > 4000/ > 125
5g	1399/ > 4000/ 62.5	1789/ > 4000/31.25
5h	1570/ > 4000/ > 31.25	916/ > 2000/250
5i	1308/ > 2000/ > 62.5	1223/ > 4000/ < 31.25
5k	2028/ > 4000/62.5	2253/ > 4000/125
6a	1780/ > 4000/ 62.5	2409/ > 4000/ < 250
6b	1916/ > 4000/ < 31.25	892/ > 2000/31.25
7a	1688/ > 4000/ < 31.25	1351/ > 4000/62.5
7b	920/ > 2000/31.25	998/ > 2000/ < 62.5
8a	1377/2000/ < 31.25	1711/ > 4000/62.5
8b	1676/ > 4000/ < 31.25	1122/ > 2000/31.25
10	1541/ > 4000/62.5	1192/ > 2000/ < 31.25
11	1658/4000/31.25	1242/ > 4000/250
12	962/ < 2000 > 62.5	1530/ > 4000/ > 125
13	1778/ > 2000/ > 31.25	1605/ > 4000/250
16	789/ > 2000/125	1044/ > 2000/125
17	732/ > 2000/ > 62.5	1003/ > 2000/31.25
18	1468/ > 4000/ > 62.5	1391/ > 2000/ < 62.5
19	1904/ > 4000/125	738/2000/ < 31.25
C+	496/ < 3000/ > 31.25	523/ < 3000/ < 62.5

[a] LD_{50} = is the amount of a compounds, which causes the death of 50% (one half) of test fungi.
[b] MFC = Minimum Fungicidal Concentration.[c] MIC = Minimum Inhibitory Concentration.
C+ = Positive control (Thiram 80%).

attack on the carbon atom result in a heterocyclization, which leads to the formation of compound **15**.[36,37]

Two separate bands (symmetrical and asymmetrical stretching bands) corresponding to the -NH_2 group were observed at 3283–3083 cm^{-1} in the IR spectra of compounds **3**, **9**, and **15**. These bands are the most significant evidence that cyclization took place. Again, in compounds **3**, **9**, and **15**, the –C=N– group stretching bands in the thiadiazole ring were observed at 1629–1600 cm^{-1}. The -NH_2 group proton signals of these compounds in the ^{1}H NMR spectra were recorded as a singlet corresponding to 2 protons in the 7.33-7.02 ppm range. Proton peaks belonging to the -NH_2 group of these compounds (**3**, **9**, and **15**) disappeared as a result of proton-deuterium exchange conducted with D_2O. The methylene (–CH_2) protons bonding the phenyl group to the thiadiazole ring from the 5-position were observed as a singlet corresponding to 2 protons in the 4.32-4.27 ppm range for compounds **3** and **9** due to the electronegative effect of the sulfur atom, and at 4.04 ppm for compound **15**. In ^{13}C NMR spectra, it was observed that resonance values belonging to C_2 and C_5 carbons of the thiadiazole ring and carbons of the substituted phenyl ring were consistent with the literature data.[35] In addition, other spectral data related to the formation of these compounds fully confirmed the proposed structures.

In the second part of the synthesis study, the first target compounds, 2,6-disubstituted imidazo[2,1-*b*][1,3,4]thiadiazole derivatives (compounds **5a–k, 10**, and **16**), were obtained from the reactions of 2-amino-1,3,4-thiadiazole derivatives (compounds **3**, **9**, and **15**) with 2-bromoacetophenone derivatives (**4a–k**) in ethanol with moderate to good yields (59% and

Table 4. Minimum inhibitory concentration (MIC) values against tested bacteria.

Compounds	Minimum Inhibitory Concentration MIC (μg/mL)		
	Cmm	*Xxv*	*Pst*
5a	100	200	50
5b	200	25	100
5c	6.25	50	50
5d	25	50	50
5e	6.25	6.25	25
5f	3.125	6.25	12.5
5g	50	6.25	25
5h	100	100	12.5
5i	200	25	50
5k	12.5	100	25
6a	200	3.125	50
6b	100	100	100
7a	200	200	100
7b	1.563	3.125	1.563
8a	100	100	200
8b	200	50	50
10	3.125	50	3.125
11	3.125	25	6.25
12	6.25	50	12.5
13	25	25	3.125
16	12.5	25	3.125
17	100	3.125	6.25
18	12.5	12.5	12.5
19	25	25	1.563

Cmm = Clavibacter michiganensis subsp. michiganensis, Xxv = Xanthomonas axonopodis pv. vesicatoria, Pst = Pseudomonas syringae pv. tomato.

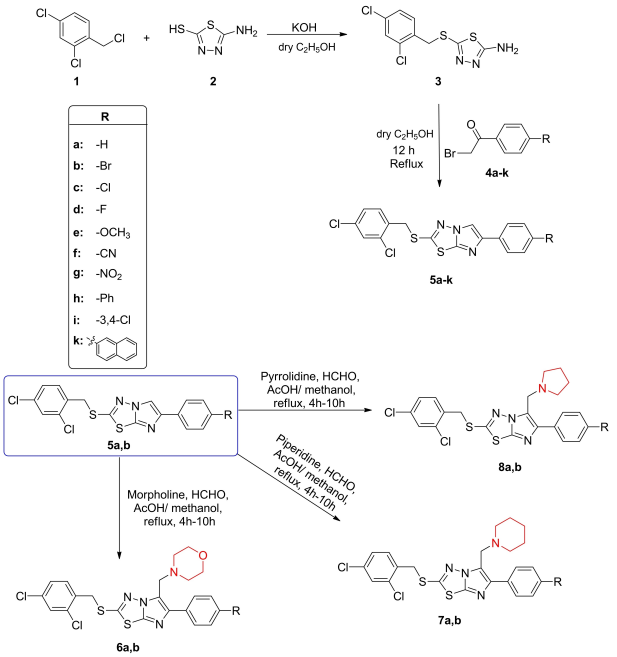

Scheme 1. Synthetic route for the synthesis of 2,6-disubstituted (**5a-k**) and 2,5,6-trisubstituted (**6a–b**, **7a–b**, **8a–b**) imidazo[2,1-*b*][1,3,4]thiadiazole derivatives.

74%) (Schemes 1–3). The proposed reaction mechanism for the formation of these compounds is shown in Scheme 4.

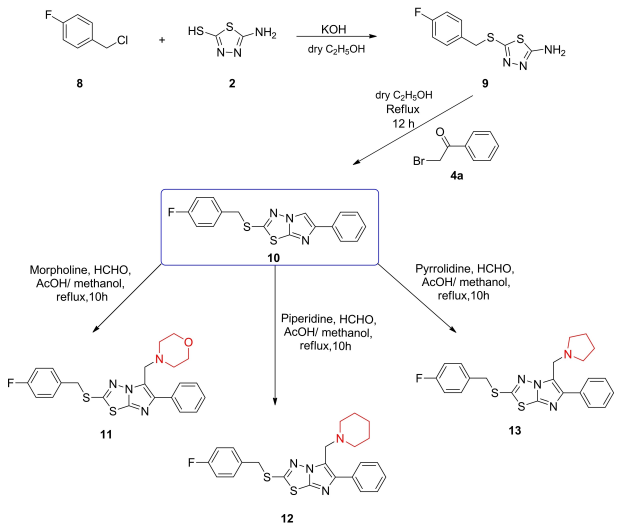

Scheme 2. Synthetic route for the synthesis of 2,6-disubstituted (**10**) and 2,5,6-trisubstituted (**11-13**) imidazo[2,1-*b*][1,3,4]thiadiazole derivatives.

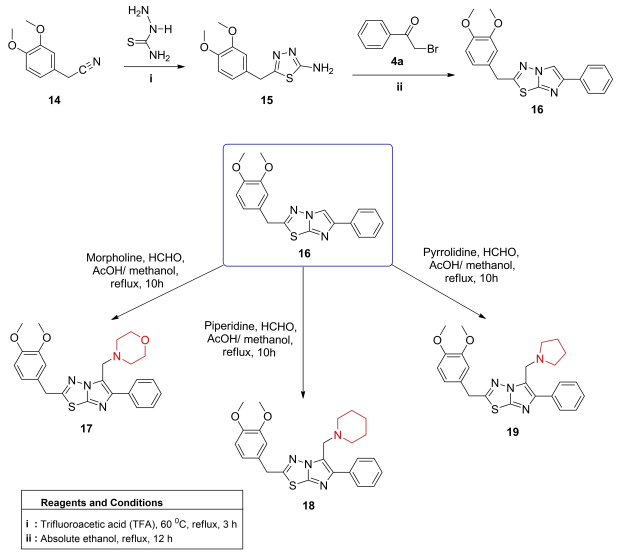

Scheme 3. Synthetic route for the synthesis of 2,6-disubstituted (**16**) and 2,5,6-trisubstituted (**17–19**) imidazo[2,1-*b*][1,3,4]thiadiazole derivatives.

The most important evidence for the formation of 2,6-disubstituted imidazo[2,1-*b*][1,3,4]thiadiazole derivatives (compounds **5a–k**, **10**, and **16**) in the IR spectra is the disappearance of the -NH_2 group symmetric and asymmetric absorption bands found for the starting compounds in the 3283–3083 cm^{-1} range.

Additionally, there are two significant indicators for the formation of these compounds in the ^{1}H NMR spectra. The first is the disappearance of the -NH_2 group proton signals corresponding to 2 protons and observed at 7.33–7.02 ppm for the 2-amino-1,3,4-thiadiazole derivatives. The second is the observation of a singlet corresponding to 1 proton in the 8.95–8.54 ppm range, representing C_5-H signals in the imidazo[2,1-*b*]

Table 5. Crystallographic data for compounds **5a-d, 6a**, and **11**.

Compounds	**5a**	**5b**	**5c**	**5d**	**6a**	**11**
Molecular formula	$C_{17}H_{11}Cl_2N_3S_2$	$C_{17}H_{10}BrCl_2N_3S_2$	$C_{17}H_1Cl_3N_3S_2$	$C_{17}H_{10}Cl_2FN_3S_2$	$C_{22}H_{22}Cl_2N_4OS_2$	$C_{22}H_{21}FN_4OS_2$
Molecular weight	392.33	471.22	426.77	410.32	491.46	440.56
Temperature/K	293(2)	296	293(2)	293(2)	293(2)	293(2)
Crystal system	triclinic	monoclinic	triclinic	triclinic	monoclinic	triclinic
Space group	P-1	$P2_1/c$	P-1	P-1	$P2_1/n$	P-1
a/Å	5.7014(3)	6.9373(6)	5.7256(7)	5.7047(4)	12.9429(15)	10.0786(8)
b/Å	8.9353(5)	7.6482(6)	9.4767(13)	9.1075(5)	11.2819(15)	10.1236(9)
c/Å	17.0253(10)	33.856(3)	17.139(2)	17.0168(10)	15.715(2)	11.4454(10)
α/°	95.534(2)	90	98.031(5)	96.371(2)	90	110.762(4)
β/°	95.283(2)	91.114(3)	95.935(4)	95.420(2)	98.854(5)	94.180(4)
γ/°	103.722(2)	90	104.139(4)	104.288(2)	90	92.776(4)
Volume/Å^3	832.70(8)	1796.0(3)	883.7(2)	844.64(9)	2267.3(5)	1085.59(16)
Z	2	4	2	2	4	2
ρcalcg/cm^3	1.565	1.7426	1.608	1.617	1.443	1.354
μ/mm^{-1}	0.644	2.824	0.760	0.647	0.493	0.275
F(000)	400.0	937.3	434.0	418.0	1020.0	464.0
Crystal size/mm^3	0.12×0.11×0.08	0.17×0.16×0.12	0.18×0.17×0.13	0.18×0.15×0.13	0.22×0.18×0.15	0.22×0.21×0.18
Radiation	MoKα (λ = 0.71073)	Mo Kα (λ = 0.71073)	MoKα (λ = 0.71073)	MoKα (λ = 0.71073)	MoKα (λ = 0.71073)	MoKα (λ = 0.71073)
2Θ range for compound data collection/°	6.342 to 49.994	6.3 to 52	6.026 to 56.65	6.246 to 56.774	6.37 to 56.986	5.844 to 49.996
Index ranges	$-6 \le h \le 6$, $-10 \le k \le 10$, $-20 \le l \le 20$	$-9 \le h \le 9$, $-10 \le k \le 10$, $-44 \le l \le 45$	$-7 \le h \le 7$, $-12 \le k \le 12$, $-22 \le l \le 22$	$-7 \le h \le 7$, $-12 \le k \le 12$, $-22 \le l \le 22$	$-14 \le h \le 17$, $-14 \le k \le 15$, $-21 \le l \le 21$	$-11 \le h \le 11$, $-12 \le k \le 12$, $-13 \le l \le 13$
Reflections collected	31231	31419	45534	46539	47416	36637
Independent reflections	2909 [R_{int} = 0.0276, R_{sigma} = 0.0132]	3540 [R_{int} = 0.0782, R_{sigma} = 0.0633]	4401 [R_{int} = 0.0393, R_{sigma} = 0.0200]	4212 [R_{int} = 0.0378, R_{sigma} = 0.0179]	5308 [R_{int} = 0.0475, R_{sigma} = 0.0312]	3778 [R_{int} = 0.0398, R_{sigma} = 0.0227]
Data/restraints/parameters	2909/147/282	3540/0/226	4401/0/226	4212/7/236	5308/0/281	3778/0/271
Goodness-of-fit on F^2	1.065	1.070	1.053	1.031	1.262	1.171
Final R indexes [I > = 2σ (I)]	R_1 = 0.0346, wR_2 = 0.0768	R_1 = 0.0883, wR_2 = 0.1935	R_1 = 0.0390, wR_2 = 0.0947	R_1 = 0.0372, wR_2 = 0.0905	R_1 = 0.0991, wR_2 = 0.1800	R_1 = 0.0567, wR_2 = 0.1352
Final R indexes [all data]	R_1 = 0.0400, wR_2 = 0.0804	R_1 = 0.1137, wR_2 = 0.2101	R_1 = 0.0485, wR_2 = 0.1031	R_1 = 0.0514, wR_2 = 0.1007	R_1 = 0.1196, wR_2 = 0.1918	R_1 = 0.0669, wR_2 = 0.1399
Largest diff. peak/hole / e Å^{-3}	0.30/−0.31	0.85/−1.28	0.34/−0.80	0.28/−0.77	0.31/−0.46	0.22/−0.64
CCDC	2009580	2009581	2009582	2009583	2009584	2009585

[1,3,4]thiadiazole derivatives. These results show good coherence with the data in the literature.[1,34,37]

The carbon signals that appeared in the 113.87-109.83 ppm range and the 146.37-145.29 ppm range in the ^{13}C NMR spectra of the imidazo[2,1-*b*][1,3,4]thiadiazole derivatives (compounds **5a–k, 10**, and **16**) are important evidence for the formation of imidazole. These signals represent the C_5 and C_6 carbons of imidazo[2,1-*b*][1,3,4]thiadiazole derivatives, respectively. Other spectral data of 2,6-disubstituted imidazo[2,1-*b*][1,3,4]thiadiazole derivatives are detailed in the experimental section.

In the final part of the synthesis study, the other target compounds, 2,5,6-trisubstituted imidazo[2,1-*b*][1,3,4]thiadiazole derivatives (compounds **6a–b**, **7a–b**, **8a–b**, **11–13**, and **17–19**), were synthesized in yields of 56% to 68%. This reaction sequence, which is a Mannich reaction, consists of the reactions of imidazo[2,1-*b*][1,3,4]thiadiazole derivatives (compounds **5a–b**, **10**, and **16)** with morpholine, piperidine, and pyrrolidine, respectively, in methanol accompanied by formalin and glacial acetic acid. The proposed reaction mechanism for the formation of the target compounds, trisubstituted imidazo[2,1-*b*][1,3,4]thiadiazole derivatives containing morpholine, piperidine, and pyrrolidine, is shown in Scheme 5.

Aromatic and aliphatic absorption bands (–CH, –C=C–, and –C=N–) similar to the 2,6-disubstituted imidazo[2,1-*b*][1,3,4] thiadiazole derivatives (compounds **5a–b**, **10**, and **16**) used in the synthesis of the Mannich bases (compounds **6a–b**, **7a–b**, **8a-b**, **11–13**, and **17–19**) were observed in the IR spectra of these compounds. All spectral data obtained in the study are given in detail in the experimental section.

A singlet corresponding to 1 proton in the 8.95-8.54 ppm range and expressing the C_5-H signals of the starting compounds, 2,6-disubstituted imidazo[2,1-*b*][1,3,4]thiadiazole derivatives (compounds **5a–b**, **10**, and **16**), disappeared in the ^{1}H NMR spectra of these Mannich bases. Instead, -NCH_2- signals were observed as a singlet corresponding to 2 protons and connecting the morpholine, piperidine, and pyrrolidine rings to the C_5 carbon in 2,5,6-trisubstituted imidazo[2,1-*b*][1,3,4]thiadiazole derivatives in the 4.02-3.74 ppm range, which is significant evidence for the formation of these compounds. These results fully confirm the proposed structures and are consistent with

Table 6. Pharmaceutical properties and binding affinities of all compounds and co-ligand.

Comp.	Binding Affinity kcal/mol	MW g/mol	ClogP	tPSA Å^2	Rotatable Bonds	Flexibility	HBD	HBA	Lipinski Violation	Solubility (mg/L)	Fsp^3	Predicted LD_{50} mg/kg	Predicted Toxicity Class
5a	−8.6	392.33	6.1	83.73	4	0.16	0	3	1	755	0.06	300	3
5b	−8.3	471.22	6.79	83.73	4	0.16	0	3	1	360	0.06	300	3
5c	−8.0	426.77	6.73	83.73	4	0.16	0	3	1	446.04	0.06	300	3
5d	−8.9	410.32	6.2	83.73	4	0.16	0	3	1	663.16	0.06	300	3
5e	−8.0	422.35	6.07	92.96	5	0.19	0	4	1	765.4	0.11	300	3
5f	−8.7	417.33	5.82	107.52	4	0.15	0	4	1	829.66	0.06	300	3
5g	−8.7	437.32	5.93	129.55	5	0.18	0	6	1	773.65	0.06	1000	4
5h	−9.0	468.42	7.73	83.73	5	0.16	0	3	1	213.13	0.04	300	3
5i	−8.6	461.22	7.36	83.73	4	0.16	0	3	1	261.8	0.06	1190	4
5k	−9.3	442.38	7.35	83.73	4	0.13	0	3	1	280.21	0.05	300	3
6a	−8.2	491.46	5.6	96.2	6	0.18	0	5	1	907.25	0.27	1000	4
6b	−7.7	570.35	6.29	96.2	6	0.18	0	5	1	417.98	0.27	1000	4
7a	−9.2	489.48	6.82	88.17	6	0.18	0	4	1	428.56	0.3	1000	4
7b	−9.5	568.38	7.51	88.17	6	0.18	0	4	1	197.55	0.3	1000	4
8a	−8.1	475.46	6.46	88.17	6	0.19	0	4	1	560.71	0.27	300	3
8b	−8.7	554.35	7.15	88.17	6	0.19	0	4	1	259.53	0.27	1000	4
10	−8.4	341.43	4.95	83.73	4	0.16	0	3	0	1859.07	0.06	300	3
11	−8.6	440.56	4.45	96.2	6	0.18	0	5	0	2301.13	0.27	1000	4
12	−8.8	438.58	5.67	88.17	6	0.18	0	4	1	1086.49	0.3	1000	4
13	−8.0	424.56	5.31	88.17	6	0.19	0	4	1	1416.65	0.27	300	3
16	−8.3	351.42	4.41	76.89	5	0.19	0	5	0	2886.69	0.16	300	3
17	−7.8	450.55	3.91	89.36	7	0.21	0	7	0	3432.65	0.33	750	4
18	−9.0	448.58	4.99	81.33	7	0.21	0	6	0	1617.13	0.36	1000	4
19	−7.9	434.55	4.77	81.33	7	0.21	0	6	0	2117.68	0.33	800	4
Co-ligand	−7.9	383.7	5.24	24.5	6	0.26	1	3	1	1838.85	0.22	1000	4

HBD: hydrogen bond donor; HBA: hydrogen bond acceptor.

Table 7. Interactions between co-ligand and 3R9C receptor.

Name	Distance Donor Acceptor (Å)	Interaction Category	Interaction Types	Donor Group	Donor Group Types	Acceptor Group	Acceptor Group Types
A:ECL451:H19-A:HIS364:O	1.97474	Hydrogen Bond	Conventional Hydrogen Bond	A:ECL451:H19	H-Donor	A:HIS364:O	H-Acceptor
A:PHE359-A:ECL451	4.65695	Hydrophobic	Pi–Pi T-shaped	A:PHE359	Pi-Orbitals	A:ECL451	Pi-Orbitals
A:ALA372-A:ECL451:CL2	3.62722	Hydrophobic	Alkyl	A:ALA372	Alkyl	A:ECL451:CL2	Alkyl
A:ECL451:CL4-A:LEU184	4.70151	Hydrophobic	Alkyl	A:ECL451:CL4	Alkyl	A:LEU184	Alkyl
A:ECL451:CL4-A:ILE255	4.82274	Hydrophobic	Alkyl	A:ECL451:CL4	Alkyl	A:ILE255	Alkyl
A:ECL451:CL4-A:LEU404	4.69536	Hydrophobic	Alkyl	A:ECL451:CL4	Alkyl	A:LEU404	Alkyl
A:ECL451:CL2-A:LEU264	3.80534	Hydrophobic	Alkyl	A:ECL451:CL2	Alkyl	A:LEU264	Alkyl
A:ECL451:CL2-A:PRO302	4.67674	Hydrophobic	Alkyl	A:ECL451:CL2	Alkyl	A:PRO302	Alkyl
A:ECL451-A:ALA256	5.27878	Hydrophobic	Pi-Alkyl	A:ECL451	Pi-Orbitals	A:ALA256	Alkyl
A:ECL451-A:VAL303	5.33539	Hydrophobic	Pi-Alkyl	A:ECL451	Pi-Orbitals	A:VAL303	Alkyl
A:ECL451-A:PRO302	5.04088	Hydrophobic	Pi-Alkyl	A:ECL451	Pi-Orbitals	A:PRO302	Alkyl
A:ECL451-A:CYS366	5.17268	Hydrophobic	Pi-Alkyl	A:ECL451	Pi-Orbitals	A:CYS366	Alkyl
A:ECL451-A:ALA372	1.97474	Hydrophobic	Pi-Alkyl	A:ECL451:H19	Pi-Orbitals	A:HIS364:O	H-Acceptor

the data in the literature.[38,39] Other ^{1}H NMR spectral data of the target compounds are detailed in the experimental section.

As expected, the chemical shifts were observed to be similar to 2,6-disubstituted imidazo[2,1-*b*][1,3,4]thiadiazole derivatives in the ^{13}C NMR spectra of the Mannich bases (compounds **6a–b**, **7a–b**, **8a–b**, **11–13**, and **17–19**). Distinctively, -NCH_2- signals connecting the morpholine, piperidine, and pyrrolidine rings to the C_5 carbon in 2,5,6-trisubstituted

Table 8. Interactions between compound **5k** and 3R9C receptor.

Name	Distance Donor Acceptor (Å)	Interaction Category	Interaction Types	Donor Group	Donor Group Types	Acceptor Group	Acceptor Group Types
d:***0:HN-A:GLY358:O	2.33401	Hydrogen Bond	Conventional Hydrogen Bond	d:***0:HN	H-Donor	A:GLY358:O	H-Acceptor
A:VAL303:CG2-d:***0	3.99203	Hydrophobic	Pi-Sigma	A:VAL303:CG2	C-H	d:***0	Pi-Orbitals
A:VAL306:CG1-d:***0	3.80563	Hydrophobic	Pi-Sigma	A:VAL306:CG1	C-H	d:***0	Pi-Orbitals
d:***0:Cl-A:LEU305	4.87776	Hydrophobic	Alkyl	d:***0:Cl	Alkyl	A:LEU305	Alkyl
d:***0-A:VAL303	4.89069	Hydrophobic	Pi-Alkyl	d:***0	Pi-Orbitals	A:VAL303	Alkyl
d:***0-A:CYS366	4.3117	Hydrophobic	Pi-Alkyl	d:***0	Pi-Orbitals	A:CYS366	Alkyl
d:***0-A:VAL303	5.36152	Hydrophobic	Pi-Alkyl	d:***0	Pi-Orbitals	A:VAL303	Alkyl
d:***0-A:ALA372	5.41691	Hydrophobic	Pi-Alkyl	d:***0	Pi-Orbitals	A:ALA372	Alkyl
d:***0-A:LEU264	5.18674	Hydrophobic	Pi-Alkyl	d:***0	Pi-Orbitals	A:LEU264	Alkyl
d:***0-A:PRO302	4.52438	Hydrophobic	Pi-Alkyl	d:***0	Pi-Orbitals	A:PRO302	Alkyl
d:***0-A:ALA372	4.22556	Hydrophobic	Pi-Alkyl	d:***0	Pi-Orbitals	A:ALA372	Alkyl

Table 9. Interactions between compound **6b** and 3R9C receptor.

Name	Distance Donor Acceptor (Å)	Interaction Category	Interaction Types	Donor Group	Donor Group Types	Acceptor Group	Acceptor Group Types
d:***0:HN-A:LEU252:O	1.71417	Hydrogen Bond	Conventional Hydrogen Bond	d:***0:HN	H-Donor	A:LEU252:O	H-Acceptor
A:LEU252:CG-d:***0	3.56519	Hydrophobic	Pi-Sigma	A:LEU252:CG	C-H	d:***0	Pi-Orbitals
A:LEU252:CD2-d:***0	3.84427	Hydrophobic	Pi-Sigma	A:LEU252:CD2	C-H	d:***0	Pi-Orbitals
A:LEU252:CD2-d:***0	3.47683	Hydrophobic	Pi-Sigma	A:LEU252:CD2	C-H	d:***0	Pi-Orbitals
A:ILE255:CD1-d:***0	3.60496	Hydrophobic	Pi-Sigma	A:ILE255:CD1	C-H	d:***0	Pi-Orbitals
A:ALA95-d:***0:Br	3.67854	Hydrophobic	Alkyl	A:ALA95	Alkyl	d:***0:Br	Alkyl
A:ALA256-d:***0:Cl	3.89244	Hydrophobic	Alkyl	A:ALA256	Alkyl	d:***0:Cl	Alkyl
d:***0:Cl-A:LEU367	3.87718	Hydrophobic	Alkyl	d:***0:Cl	Alkyl	A:LEU367	Alkyl
d:***0:Cl-A:CYS366	4.4033	Hydrophobic	Alkyl	d:***0:Cl	Alkyl	A:CYS366	Alkyl
d:***0:Br-A:LEU180	3.86625	Hydrophobic	Alkyl	d:***0:Br	Alkyl	A:LEU180	Alkyl
d:***0-A:ILE255	5.15903	Hydrophobic	Pi-Alkyl	d:***0	Pi-Orbitals	A:ILE255	Alkyl
d:***0-A:ALA256	4.9619	Hydrophobic	Pi-Alkyl	d:***0	Pi-Orbitals	A:ALA256	Alkyl
d:***0-A:CYS366	4.83371	Hydrophobic	Pi-Alkyl	d:***0	Pi-Orbitals	A:CYS366	Alkyl
d:***0-A:LEU184	5.41959	Hydrophobic	Pi-Alkyl	d:***0	Pi-Orbitals	A:LEU184	Alkyl

imidazo[2,1-*b*][1,3,4]thiadiazole derivatives were observed in the 51.77-47.55 ppm range.

Additionally, the mass spectra of all compounds synthesized in this study were observed to be as expected and supported by molecular ion peaks. The ^{1}H NMR, ^{13}C NMR, FT-IR, mass spectroscopy, and elemental analysis data for all synthesized compounds are given in detail in the experimental section and relevant spectra are given in the supporting information section.

3. Antimicrobial Activity Studies

3.1. In Vitro Antifungal Activity Studies

In antifungal activity studies, 2000 and 4000 μg/mL doses of the compounds were tested for each fungus type. Table 1 shows the mycelium growths of the fungi and Table 2 shows the mycelium growth inhibition values. When the mycelium growths of the fungi were compared with the negative control, the *Rhizoctonia solani* pathogen was found to be the most susceptible fungus species to the tested doses. All compounds displayed antifungal activity against the fungus species tested. Mycelium growth of 60 mm was observed in DMSO (negative control) and it was found that DMSO did not prevent the growth of fungi. No mycelium growth was observed in the

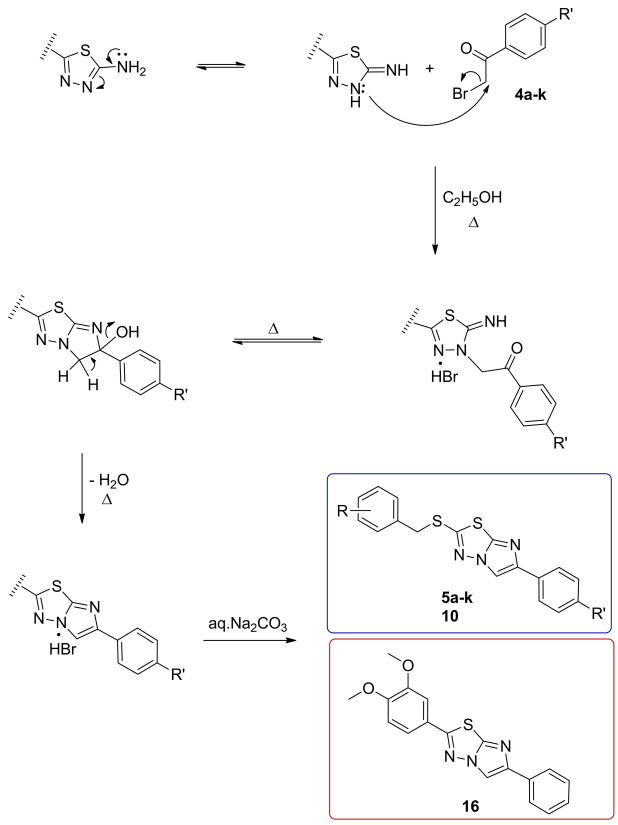

Scheme 4. Mechanism for the formation of 2,6-disubstituted imidazo[2,1-*b*][1,3,4]thiadiazole derivatives (**5a–k**, **10**, and **16**).

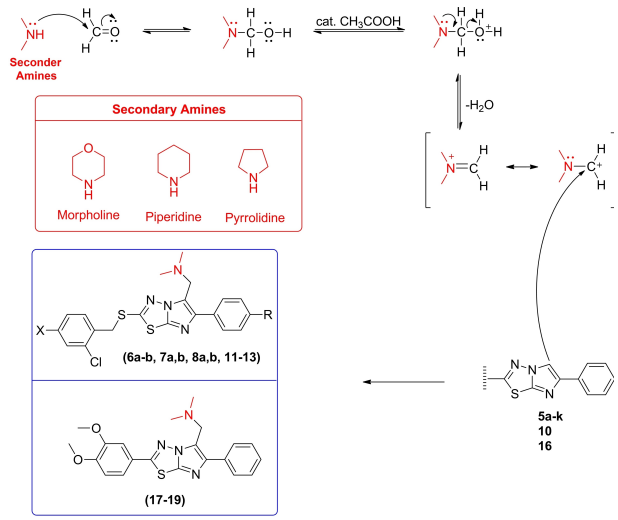

Scheme 5. Formation mechanism of the target compounds (Mannich bases) via morpholine, piperidine, and pyrrolidine.

positive control (80% thiram). At doses of 4000 μg/mL, compound **5b** showed the greatest effect against *R. solani* with 6.1 mm of mycelium growth, whereas compound **19** showed the greatest effect against *Alternaria alternata* with 6.1 mm of mycelium growth. Additionally, the mycelial growth inhibition value of the compounds against the pathogens at a dose of 4000 μg/mL was between 90% and 72% for *R. solani* and between 90% and 56% for *A. alternata*. According to these results, each compound appears to be over 50% effective against the fungi.

Similarly, the minimum fungicidal concentration (MFC), the minimum inhibition concentration (MIC), and the lethal dose (LD_{50}) values of the fungi against the compounds were calculated (Table 3). The MIC is, here, described as the lowest test concentration that does not allow detectable mycelial growth while MFC is the lowest test concentration that does not allow mycelial growth in agar. Also, the LD_{50} value corresponds to the compound dose that causes the death of 50% of the fungi tested.[40]

As shown in Table 3, the MIC values were in the range of $<$31.25 to $<$500 μg/mL for *R. solani* and $<$31.25 to 250 μg/mL for *A. alternata*. The MFC values were observed to be in the range of $>$4000 to 2000 μg/mL for both pathogens. The LD_{50} values were between 664 and 2028 μg/mL for *R. solani* and between 738 and 2981 μg/mL for *A. alternata*. These results show that the tested compounds both have a moderate to good degree of activity against each type of pathogen and can be considered as alternative fungicides against each species of fungus.

3.2. In Vitro Antibacterial Activity Studies

The MIC values of the synthesized compounds against 3 different plant pathogenic bacterial cultures (*Clavibacter michiganensis* subsp. *michiganensis*, *Xanthomonas axonopodis* pv. *vesicatoria*, *Pseudomonas syringae* pv. *tomato*) were determined in in vitro antibacterial activity studies.

Table 3 shows the MIC values of the doses prepared at concentrations of 10% (1000 μg/mL) of the compounds for *Clavibacter michiganensis* subsp. *michiganensis*, *Xanthomonas axonopodis* pv. *vesicatoria*, and *Pseudomonas syringae* pv. *tomato*. The MIC values were observed to vary for each pathogen depending on the compound's concentration (Table 4). The final concentrations of the compounds in the 12 wells used to determine the MIC values were 200 μg/mL, 100 μg/mL, 50 μg/mL, 25 μg/mL, 12.5 μg/mL, 6.25 μg/mL, 3.125 μg/mL, 1.5625 μg/mL, 0.1783 μg/mL, 0.3906 μg/mL, 0.1953 μg/mL, and 0.00 μg/mL (control), respectively. The highest MIC values for *Clavibacter michiganensis* subsp. *michiganensis* were observed for compounds **5b**, **5i**, **6a**, **7a**, and **8b** at 200 μg/mL and the lowest MIC value was observed for compound **7b** at 1.5625 μg/mL. The highest MIC values for *Xanthomonas axonopodis* pv. *vesicatoria* were observed for compounds **5a** and **7a** at 200 μg/mL and the lowest MIC value was observed for compound **7b** at 3.125 μg/mL. The highest MIC value for *Pseudomonas syringae* pv. *tomato* was observed for compound **8a** at 200 μg/mL and the lowest MIC values were observed for compounds **7b** and **19** at 1.5625 μg/mL. According to these results, the compound with the highest activity against the bacterial species was compound **7b**. The bacterial species most affected by the compounds was Xxv, followed by Cmm and Pst (Table 4).

3.3. Crystallographic Analysis

Single crystals of compounds **5a–d**, **6a**, and **11** were obtained in this study and their structures were confirmed by X-ray analysis. None of the crystals had the classical hydrogen bond and the packaging of the crystals occurred through weak van der Waals and π-π interactions. Disorder was observed in the entire 2,4-dichlorobenzyl ring of the **5a** crystal and in the Cl atom at position 4 of the **5d** crystal. Table 5 shows the data related to crystals of the compounds (**5a–d**, **6a**, and **11**) and Figure 1 shows the ORTEP diagrams.

3.4. Molecular Docking and Calculation of Physicochemical and ADME Properties

Table 6 shows the molecular weight (MW), polar surface area (tPSA), bond properties, flexibility, solubility, toxicity characteristics, indicator of lipophilicity (ClogP), Fsp^3 (fraction of saturated carbons), and violation of Lipinski's rules (Ro5)[41] for all compounds. In here, the Ro5 rules were developed by Lipinski et al. as a guide to the design of molecules that can be used orally, and it well established that the Ro5 rules had a notable impact on drug discovery strategies. In this context, the four key parameters of the Ro5 rules for the all compounds are as follows,

- A molecular weight (MW) below 500 g/mol,
- A calculated octanol-water coefficient (CLogP) smaller than 5,
- No more than 5 hydrogen bond donors,
- No more than 10 hydrogen bond acceptors.

The results showed that most of the experimentally active compounds, particularly compounds **10**, **11**, and **16–19**, comply with Lipinski's rules. This indicates the drug similarity of the compounds. Herein, another important value is the topological polar surface area (tPSA) (recommended value of ≤ 140 Å^2)[42] and this value was within the recommended range for all compounds. Also, we analyzed computed the oral toxicity level for all compounds, and compounds **5g**, **5i**, **6a**, **6b**, **7a**, **7b**, **8b**, **11**, **12**, **17**, **18**, and **19** (LD_{50} of 1000 mg/kg) were classified as class 4 toxic while the remaining compounds were classified as class 3 toxic (1: most toxic and 6: safe).[43] This situation suggests that the 12 compounds with lower toxicity values may be supposed as new drug candidates for in vitro studies. On the other hand, Fsp^3 is a newer index indicating drug similarity[44] and CLogP is a key physicochemical parameter and used to predict absorption properties in the drug discovery process.[45] It has been reported that the lower CLogP and higher Fsp^3 lead to better drug-likeness properties.[46]

In addition to the pharmacological properties of all molecules, the binding affinity values of the molecules were calculated by using molecular docking simulations Autodock Vina[47] open-source program with Lamarckian genetic algorithm.[48,49] In molecular docking studies, the crystal structure (PDB ID: 3R9C) of *Mycobacterium smegmatis* CYP164 A2, which forms a complex with the structure of the antifungal drug econazole, was used. Therefore, econazole molecule was evaluated as a co-ligand in this study. By using the protein and ligand preparation wizards in the PyRx package,[50] we prepared the 3R9C receptor and all compounds for docking operations. Then, docking operations were carried out for these complexes and the obtained values were added in Table 1. It is seen from the Table1 that **5k** (−9.3 kcal/mol) and **7b** (−9.5 kcal/mol) compounds, which were observed to be effective in vitro studies, have the highest binding affinity values. Also, the synthesized all compounds except **6b** (−7.7 kcal/mol), **17** (−7.8 kcal/mol), and **19** (-7.9 kcal/mol) have higher affinity value than econazole (−7.9 kcal/mol) as co-ligand.

Furthermore, we also depicted the molecular interactions between the 3R9C receptor and two compounds with the highest affinity (**5k** and **7b**), one compound with the lowest affinity (**6b**) and econazole molecule as a co-ligand in Figures 2–4. Figure 2 shows a three-dimensional (3D) representation of the molecular interaction of co-ligand and compounds **5k**, **6b**, and **7b** while Figure 3 represent their two-dimensional (2D) interaction diagrams. From the Figures, it can be clearly

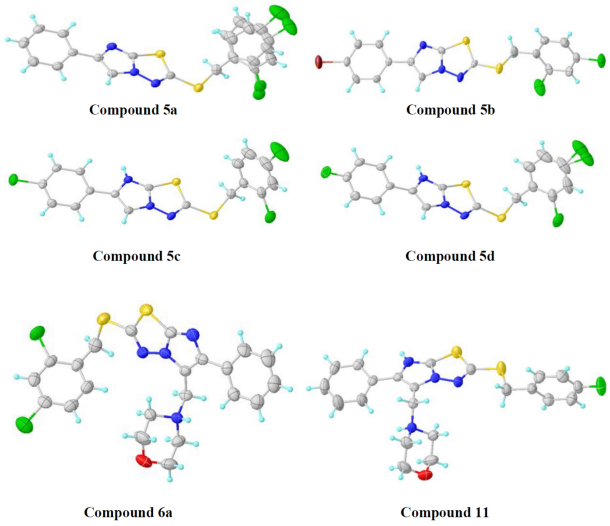

Figure 1. The crystal structures of compounds **5a–d**, **6a**, and **11**.

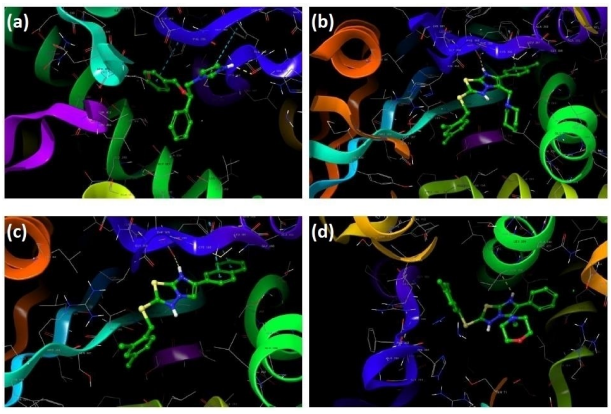

Figure 2. The 3D interactions between 3R9C receptor and (a) econazole, (b) **7b**, (c) **5k**, and (d) **6b** compounds.

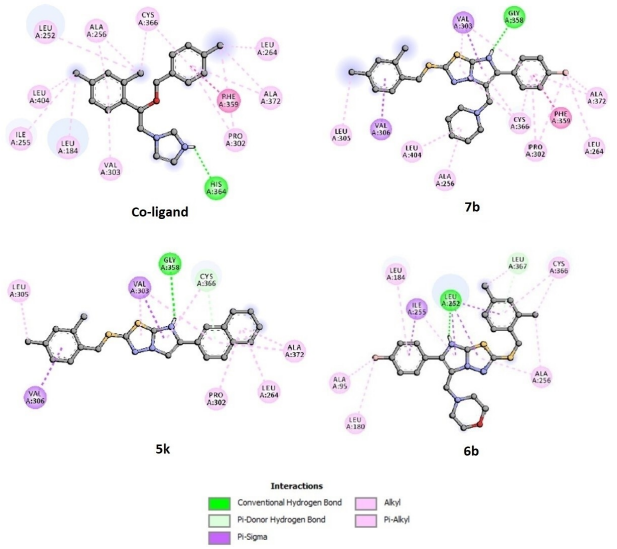

Figure 3. The 2D interaction diagram between 3R9C receptor and econazole, **5k**, **6b**, and **7b** compounds.

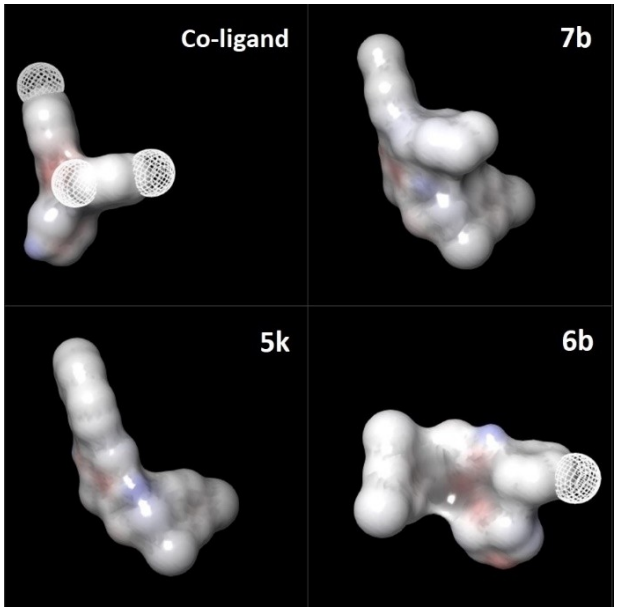

Figure 4. Binding surface of the target together with econazole, **5k**, **6b**, and **7b** compounds.

observed the active binding sites of the co-ligand to the target protein. As it is clearly seen in the Figure 3, many common interactions are seen between the residues (PRO302, LEU 305, LEU264, ALA372, VAL303, VAL306 and GLY358) of the 3R9C and the compounds **5k** and **7b** with high affinity.

Moreover, compounds **5k** and **7b** with higher docking scores as shown in Figure 4 had a similar parallel orientation with the co-ligand at the active site of the receptor, while compound **6b** with a lower docking score had a perpendicular orientation compared to co-ligand and the compounds **5k** and **7b**.

Finally, Tables 7–10 show the interaction types and distances between the ligands and the receptor in detailed. According to these Tables, the co-ligand was observed to have a classic (conventional) hydrogen bond interaction with the HIS364 residue in the active binding site of the receptor. Also, compounds **5k** and **7b** have a classic hydrogen with GLY358 residue while compound **6b** was observed to have a classic hydrogen bond interaction with the LEU252 residue.

4. Conclusion

In this study, 2,6-disubstituted and 2,5,6-trisubstituted imidazo [2,1-*b*][1,3,4]thiadiazole derivatives, the target compounds, were synthesized using simple and applicable reaction conditions. The structures of all synthesized compounds were analyzed using by various techniques (^{1}HNMR, ^{13}CNMR, FT-IR, elemental analysis, mass spectroscopy, and X-ray diffraction).

In vitro antifungal and antibacterial activity tests were performed for the target compounds against various plant pathogens. According to the results of the tests, most of the compounds had moderate to good antifungal and antibacterial activities against the plant pathogens. Other active groups (morpholine, piperidine, and pyrrolidine) were used together with bioactive compounds such as imidazole and thiadiazole and the effect of these groups on biological activity was determined with this study. The antibacterial activity studies particularly showed that the compounds containing morpholine and piperidine significantly increased the activity. The most active compound for all species of bacteria and fungi in biological activity studies was found to be compound **7b**, containing the piperidine group.

In molecular docking studies, we have observed that all compounds had higher docking scores than econazole, the inhibitor of 3R9C receptor, and had also similar interactions to econazole. Also, it was noticed that compounds **5k** and **7b**, which showed antibacterial properties in experimental studies, have the highest docking score (-9.5 and −9.3 kcal/mol, respectively). Furthermore, it was determined that compounds **10**, **11**, and **16**–**19** complied with Lipinski's rules.

5. Crystallographic Data

Deposition Numbers 2009580 (**5a**), 2009581 (**5b**), 2009582 (**5c**), 2009583 (**5d**), 2009584 (**6a**), and 2009585 (**11**) contains the supplementary crystallographic data for this paper. These data are provided free of charge by the joint Cambridge Crystallographic Data Centre and Fachinformationszentrum Karlsruhe Access Structures service www.ccdc.cam.ac.uk/structures.

Supporting Information Summary

The supporting information contains details of the experimental procedures (synthetic, biological, and theoretical) and spectral characterization data (^{1}H NMR, ^{13}C NMR, FT-IR, and Mass Spectra) for all compounds.

Acknowledgments

The authors would like to thank the funding support from Karabuk University (KBU-BAP-15/2-YL-018).

Conflict of Interest

The authors declare no conflict of interest.

Keywords: Ab initio calculations · ADME · Biological activity · Imidazo[2,1-*b*][1,3,4]thiadiazole · Mannich bases

[1] H. Tahtaci, H. Karacık, A. Ece, M. Er, M. G. Şeker, *Mol. Inf.* **2018**, *37*, 1700083.
[2] A. K. Singh, G. Mishra, K. Jyoti, *J. Appl. Pharm. Sci.* **2011**, *01*, 44–49.
[3] M. L. Fascio, C. S. Sepulveda, E. B. Damonte, N. B. D'Accorso, *Carbohydr. Res.* **2019**, *480*, 61–66.
[4] S. Cascioferro, G. L. Petri, B. Parrino, D. Carbone, N. Funel, G. Mantini, H. Dekker, D. Geerke, G. J. Peters, G. Cirrincione, E. Giovannetti, P. Diand, *Eur. J. Med. Chem.* **2020**, *189*, 112088.
[5] K. Viprabha, K. D. Udaya, P. P. Nikhil, C. Keloth, *Dyes Pigm.* **2019**, *167*, 216–224.
[6] M. Petrusova, H. Smrticova, B. Pribulova, S. Vlckova, I. Uhliarikova, T. Dosca, L. Somsak, L. Petrus, *Tetrahedron* **2016**, *72*, 2116–2121.
[7] S. J. Singh, S. Rajaminickam, A. Gogoi, B. K. Patel, *Tetrahedron Lett.* **2016**, *57*, 1044–1047.
[8] D. M. Egorov, Y. L. Piterskaya, A. V. Dogadina, N. I. Svintsitskaya, *Tetrahedron Lett.* **2015**, *56*, 1552–1554.
[9] L. Strzemecka, Z. Urbanczyk-Lipkowska, *J. Mol. Struct.* **2010**, *970*, 1–13.
[10] R. Yi, S. Liu, H. Gao, Z. Liang, X. Xu, N. Li, *Tetrahedron* **2020**, *76*, 130951.
[11] U. Kalidhar, R. Kumar, A. Kaur, *Res. J. Pharm. Biol. Chem. Sci.* **2012**, *3*, 1072.
[12] W. S. Alwan, R. Karpoormath, M. B. Palkar, H. M. Patel, R. A. Rane, M. S. Shaikh, A. Kajee, K. P. Mlisana, *Eur. J. Med. Chem.* **2015**, *95*, 514–525.
[13] I. A. M. Khazi, A. K. Gadad, R. S. Lamani, B. A. Bhongade, *Tetrahedron* **2011**, *67*, 3289–3316.
[14] A. K. Gadad, C. S. Mahajanshetti, S. Nimbalkar, A. Raichurkar, *Eur. J. Med. Chem.* **2000**, *35*, 853–857.
[15] T. M. Gireesh, R. R. Kamble, T. Taj, *Pharm. Chem. J.* **2011**, *45*, 313–316.
[16] S. G. Alegaon, K. R. Alagawadi, *Eur. J. Chem.* **2011**, *2*, 94–99.
[17] Y. Luo, S. Zhang, Z. J. Liu, W. Chen, J. Fu, Q. F. Zeng, H. L. Zhu, *Eur. J. Med. Chem.* **2013**, *64*, 54–61.
[18] B. Chandrakantha, A. M. Isloor, P. Shetty, H. K. Fun, G. Hedge, *Eur. J. Med. Chem.* **2014**, *71*, 316–323.
[19] K. F. M. Atta, O. O. M. Farahat, A. Z. A. Ahmed, M. G. Marei, *Molecules* **2011**, *16*, 5496–5506.
[20] A. A. Kadi, N. R. El-Brollosy, O. A. Al-Deeb, E. E. Habib, T. M. Ibrahim, A. A. El-Emam, *Eur. J. Med. Chem.* **2007**, *42*, 235–242.
[21] A. K. Gadad, M. B. Palkar, K. Anand, M. N. Noolvi, T. S. Boreddy, J. Wagwade, *Bioorg. Med. Chem.* **2008**, *16*, 276–283.
[22] V. B. Jadhav, M. V. Kulkarni, V. P. Rasal, S. S. Biradar, M. D. Vinay, *Eur. J. Med. Chem.* **2007**, *43*, 1721–1729.
[23] J. Ramprasad, N. Nayak, U. Dalimba, P. Yogeeswari, D. Sriram, *Bioorg. Med. Chem. Lett.* **2015**, *25*, 4169–4173.
[24] J. Ramprasad, N. Nayak, U. Dalimba, P. Yogeeswari, D. Sriram, S. K. Peethambar, R. Achur, H. S. Kumar, *Eur. J. Med. Chem.* **2015**, *95*, 49–63.
[25] S. G. Alegaon, K. R. Alagawadi, P. V. Sonkusare, S. M. Chaudhary, D. H. Dadwe, A. S. Shah , *Bioorg. Med. Chem. Lett.* **2012**, *22*, 1917–1921.
[26] A. K. Gadad, M. N. Noolvi, R. V. Karpoormath, *Bioorg. Med. Chem.* **2004**, *12*, 5651–5659.
[27] R. J. Roskoski, *Pharmacol. Res.* **2015**, *100*, 1–23.
[28] L. L. Corre, A. L. Girard, F. Radvanyi, C. B. Lasselin, A. Jonguoy, E. Mugniery, L. L. Mallet, P. Busca, Y. L. Merrer, *Org. Biomol. Chem.* **2010**, *8*, 2164–2173.
[29] F. Arshad, M. F. Khan, W. Akhtar, M. M. Alam, L. M. Nainwal, S. K. Kaushik, M. Akhter, S. Parvez, S. M. Hasan, M. Shaquiquzzaman, *Eur. J. Med. Chem.* **2019**, *167*, 324–356.
[30] S. Jana, S. Sarkar, S. A. Morris, *Tetrahedron* **2020**, *76*, 131215.
[31] P. Niedziałkowski, E. Czaczyk, J. Jarosz, A. Wcisło, W. Białobrzeska, J. Wietrzyk, T. Ossowski, *J. Mol. Struct.* **2019**, *1175*, 488–495.
[32] T. Ince, R. Serttas, B. Demir, H. Atabey, N. Seferoglu, S. Erdogan, E. Sahin, S. Erat, Y. Nural, *J. Mol. Struct.* **2020**, *1217*, 128400.
[33] D. T. Gerokonstantis, A. Nikolaou, C. Magkrioti, A. Afantitis, V. Aidinis, G. Kokotos, P. Moutevelis-Minakakis, *Bioorg. Med. Chem.* **2020**, *28*, 115216.
[34] M. Er, A. Özer, Ş. Direkel, T. Karakurt, H. Tahtaci, *J. Mol. Struct.* **2019**, *1194*, 284–296.
[35] M. Er, G. Isildak, H. Tahtaci, T. Karakurt, *J. Mol. Struct.* **2016**, *1110*, 102–113.
[36] M. Er, F. Ahmadov, T. Karakurt, Ş. Direkel, H. Tahtaci, *ChemistrySelect* **2019**, *4*, 14281-14290.
[37] M. Er, B. Ergüven, H. Tahtaci, A. Onaran, T. Karakurt, A. Ece, *Med. Chem. Res.* **2017**, *26*, 615–630.
[38] G. Kolavi, V. Hegde, I. A. Khazi, P. Gadad, *Bioorg. Med. Chem. Lett.* **2006**, *14*, 3069–3080.
[39] H. M. Patel, M. N. Noolvi, A. Goyal, B. S. Thippeswamy, *Eur. J. Med. Chem.* **2013**, *65*, 119–133.
[40] K. S. Babu, X. C. Li, M. R. Jacob, Q. Zhang, S. I. Khan, D. Ferreira, A. M. Clark, *J. Med. Chem.* **2006**, *49*, 7877–7886.
[41] C. A. Lipinski, F. Lombardo, B. W. Dominy, P. J. Feeney, *Adv. Drug Delivery Rev.* **1997**, *23*, 3–25.
[42] D. F. Veber, S. R. Johnson, H.-Y. Cheng, B. R. Smith, K. W. Ward, K. D. Kopple, *J. Med. Chem.* **2002**, *45*, 2615–2623.
[43] B. Rashidieh, Z. Madani, M. K. Azam, S. K. Maklavani, N. R. Akbari, S. Tavakoli, G. Rigi, *Bioinformatics* **2015**, *11*, 501–505.
[44] F. Lovering, J. Bikker, C. Humblet, *J. Med. Chem.* **2009**, *52*, 6752–6756.
[45] C. A. Lipinski, *J. Pharmacol. Tox. Met.* **2000**, *44*, 235–249.
[46] P. N. Collier, D. Messersmith, A. Le Tiran, U. K. Bandarage, C. Boucher, J. Come, K. M. Cottrell, V. Damagnez, J. D. Doran, J. P. Griffith, S. Khare-Pandit, E. B. Krueger, M. W. Ledeboer, B. Ledford, Y. Liao, S. Mahajan, C. S. Moody, S. Roday, T. Wang, J. Xu, A. M. Aronov, *J. Med. Chem.* **2015**, *58*, 5684–5688.
[47] O. Trott, A. J. Olson, *J. Comput. Chem.* **2010**, *31*, 455–461.
[48] F. J. Solis, R. J.-B. Wets, *Math. Oper. Res.* **1981**, *6*, 19–30.
[49] R. Huey, G. M. Morris, A. J. Olson, D. S. Goodsell, *J. Comput. Chem.* **2007**, *28*, 1145–1152.
[50] S. Dallakyan, A. J. Olson in *Methods Mol. Biol.*, Vol. 1263 (Eds.: J. Hempel, C. Williams, C. Hong), Springer, New York, **2015**, pp. 243–250.

Submitted: July 15, 2020
Accepted: September 28, 2020